change in the geometry of the mixed-chelate Cr(III) complexes at their LF excited state.

On the other hand, the homochelate complexes $[Cr(ox)_3]^{3-}$ and $[Cr(phen)_3]^{3+}$ are expected to expand isotropically when excited to the quartet state, since all of the six Cr(III)–ligand bonds are equivalent to a good approximation. Therefore, the inversion in the direction of the equilibrium shift is not anticipated for these homochelate complexes, as is really the case (Table II), but the optical yield attained might be changed upon photoexcitation because of their isotropic expansion at the quartet state (compare the percentage resolutions attained for $[Cr(ox)_3]^{3-}$ at the ground state with those at the excited state).

Recently, some evidence has been presented suggesting that photoreaction of some Cr(III) complexes proceeds not only from the quartet state but also from the doublet states,[27] which are designated simply as the ^2E state here, and in particular, photoaquation of $[Cr(bpy)_3]^{3+}$ is believed to occur only at the doublet ^2E state.[23b,28] Photophysical and photochemical similarities[12,29,30] between $[Cr(bpy)_3]^{3+}$ and $[Cr(phen)_3]^{3+}$ imply that photoracemization of $[Cr(phen)_3]^{3+}$ as well as $[Cr(bpy)_3]^{3+}$ might take place at the ^2E state. Since the ^2E state has the same electronic configuration ($(t_{2g})^3$) as the ground state, these two states in Cr(III) complexes have virtually the same geometry.[12,23b,24] As a result, the direction of the equilibrium shift is expected not to be inverted for $[Cr(phen)_3]^{3+}$ upon photoexcitation even if only the ^2E state is a photoreactive level. In this way, our experimental results obtained for this complex are well interpreted equally by the doublet and quartet reactivity hypotheses. However, the photochemical behavior exhibited by the mixed-chelate complexes seems not to be accounted for by the doublet reactivity hypothesis alone.

Finally, it is worth noting that Kane-Maguire et al.[31] have reported only one example, to our knowledge, in which the Pfeiffer effect is applied to partial photoresolution of $[Cr(phen)_3]^{3+}$ with ((*R*,*R*)-tartrato)antimonate(III) as an environment substance in water. The direction of the equilibrium shift they attained under photoexcitation at the LF regions is the same (Δ) as that found in the usual Pfeiffer effect of labile $[Ni(phen)_3]^{2+}$ or $[Cd(phen)_3]^{2+}$.[32] This observation is consistent with our interpretation presented above.

Acknowledgment. The present work was partially supported by a grant-in-aid for scientific research from the Ministry of Education, Science and Culture of Japan (Scientific Research No. 554188).

Registry No. $[Cr(ox)_3]^{3-}$, 15054-01-0; $[Cr(ox)_2(phen)]^-$, 21748-33-4; $[Cr(ox)_2(bpy)]^-$, 21748-32-3; $[Cr(ox)(phen)_2]^+$, 32626-76-9; $[Cr(phen)_3]^{3+}$, 15276-16-1; *d*-cinchonine hydrochloride, 5949-11-1; *l*-cinchonidine hydrochloride, 524-57-2; *d*-quinidine hydrochloride, 1668-99-1; *l*-quinine hydrochloride, 130-89-2.

(27) For example, A. R. Gutierrez and A. W. Adamson, *J. Phys. Chem.*, **82**, 902 (1978); Y. S. Kang, F. Castelli, and L. S. Forster, *ibid.*, **83**, 2368 (1979); R. T. Walters and A. W. Adamson, *Acta Chem. Scand., Ser. A*, **A33**, 53 (1979).
(28) M. A. Jamieson, N. Serpone, M. S. Henry, and M. Z. Hoffman, *Inorg. Chem.*, **18**, 214 (1979); R. L. P. Sasseville and C. H. Langford, *ibid.*, **19**, 2850 (1980).
(29) N. Serpone, M. A. Jamieson, M. S. Henry, M. Z. Hoffman, F. Bolletta, and M. Maestri, *J. Am. Chem. Soc.*, **101**, 2907 (1979); R. Sriram, M. Z. Hoffman, M. A. Jamieson, and N. Serpone, *ibid.*, **102**, 1754 (1980).
(30) N. Serpone and M. A. Jamieson, *J. Chem. Soc., Chem. Commun.*, 1006 (1980); N. A. P. Kane-Maguire, R. C. Kerr, and J. R. Walters, *Inorg. Chim. Acta*, **33**, L163 (1979).
(31) N. A. P Kane-Maguire, B. Dunlop, and C. H. Langford, *J. Am. Chem. Soc.*, **93**, 6293 (1971).
(32) L. A. Mayer and R. C. Brasted, *J. Coord. Chem.*, **3**, 85 (1973).

Contribution from the Department of Chemistry, McMaster University, Hamilton, Ontario, Canada L8S 4M1

Electronic Structure of $Zr(BH_4)_4$ and $Hf(BH_4)_4$ Studied by Photoelectron Spectroscopy and LCAO-HFS Calculations

ADAM P. HITCHCOCK,* NGUYEN HAO, NICK H. WERSTIUK, MICHAEL J. McGLINCHEY, and TOM ZIEGLER

Received February 2, 1981

The He I ultraviolet photoelectron spectra of $Zr(BH_4)_4$ and $Hf(BH_4)_4$ have been recorded and analyzed with the aid of an LCAO-HFS(Xα) calculation on $Zr(BH_4)_4$. The PE spectra of these two species are found to be essentially identical, as previously observed by Downs et al. [*J. Chem. Soc., Dalton Trans.* **1978**, 1755]. Our assignments differ in some aspects from those given previously. A qualitative scheme for the triple-bridge bonding in these molecules has been developed, which is based on an analogy with the bonding in classical d^0 tetrahedral complexes such as $TiCl_4$ and MnO_4^-. The factors determining the relative stabilities of mono-, di-, and tribridged borohydride ligands are also discussed.

Introduction

The tetrakis(tetrahydroborates) of zirconium and hafnium are volatile, covalently bonded molecular complexes, which pose interesting bonding questions. Vibrational spectroscopy,[1] electron[2,3] and neutron diffraction[4] studies, and X-ray crystallography[5] have shown that these molecules are tetrahedral with three hydrogen atoms bridging the metal atom and each boron atom. Vibrational spectroscopic studies indicate that the tetrakis(tetrahydroborates) of uranium[6] and neptunium[7] are also tetrahedral and triply bridged in the gas phase. It is also probable that tetrahydroborate derivatives of samarium[8] and thorium[9] are triply bridged.

(1) James, B. D.; Nanda, R. K.; Wallbridge, M. G. H. *J. Chem. Soc. A* **1966**, 182.
(2) Spiridonov, V. P.; Mamowa, G. I. *J. Struct. Chem.* (*Engl. Transl.*) **1969**, *10*, 120.
(3) Plato, V.; Hedberg, K. *Inorg. Chem.* **1971**, *10*, 590.
(4) Bernstein, E. R.; Hamilton, W. C.; Keiderling, T. A.; Kennelly, W. J.; LaPlaca, S. J.; Lippard, S. J.; Marks, T. J.; Mayerle, J. J., unpublished data reported in ref 13.
(5) Bird, P. H.; Churchill, M. R. *Chem. Commun.* **1967**, 403.
(6) James, B. D.; Smith, B. E.; Wallbridge, M. G. H. *J. Mol. Struct.* **1972**, *14*, 327.
(7) Banks, R. H.; Edelstein, N. *J. Chem. Phys.* **1980**, *73*, 3589.
(8) Marks, T. J.; Grynkewich, G. W. *Inorg. Chem.* **1976**, *15*, 1302.

0020-1669/82/1321-0793$01.25/0

Proton,[1,10] boron,[1] and zirconium[11] NMR studies of $Zr(BH_4)_4$ have convincingly shown that the bridging and terminal hydrogens of each BH_4 moiety are undergoing extremely rapid exchange. The NMR evidence suggests that these complexes can be viewed as a metal atom surrounded by four rapidly spinning BH_4 groups. With this outlook, the reason that the configuration is triply rather than doubly or singly bridged is not immediately obvious. We note that a plethora of metal–BH_4 complexes are known (e.g., $Al(BH_4)_3$, $Cp_2Zr(BH_4)_2$) in which the tetrahydroborate ligand is doubly bridged. The general area of transition-metal tetrahydroborates has recently been reviewed,[12,13] and the molecular dynamics of such compounds have been comprehensively discussed by Marks.[14]

In order to investigate the electronic structure of the triply hydrogen-bridged tetrahydroborate complexes, we have recorded the photoelectron spectra of $Zr(BH_4)_4$ and $Hf(BH_4)_4$ using He I radiation ($h\nu$ = 21.22 eV). The He I and He II spectra of a series of metal tetrahydroborates including $Zr(BH_4)_4$ and $Hf(BH_4)_4$ have previously been recorded by Downs et al.[15] The spectra reported herein confirm the general features of the earlier recorded spectra[15] although there are differences in the relative intensities of features, presumably caused by different spectrometer transmission characteristics. More significantly some aspects of our spectral assignments differ from those of Downs et al.[15] Our spectral analysis and qualitative description of the bonding in these complexes have been aided by comparison with the results of an LCAO–HFS($X\alpha$) calculation on $Zr(BH_4)_4$. The utility of this method for calculation of the physical properties of transition-metal complexes has recently been demonstrated.[16] This method uses the $X\alpha$ exchange potential approximation to circumvent evaluation of the multicenter integrals that make the ab initio Hartree–Fock procedure too expensive in computation time for application to large systems with realistic basis sets. In the present method the HFS equations are solved without recourse to the muffin-tin approximation to the potential that is known to deviate considerably from the true molecular potential.[17] Instead an LCAO approach is used with expansion of one-electron molecular orbitals in terms of Slater-type orbitals. The HFS equations are solved by application of the discrete variation method. Full details of this procedure have been described previously.[16]

Experimental Section

The He I photoelectron spectra were obtained with a recently developed noncommercial instrument constructed from the design of Frost et al.[18] It is based on a 10-cm diameter aluminum hemispherical electrostatic energy analyzer. The ionization region is connected directly to a 4-in. diffusion pump to allow high sample throughput for transient PES studies. For the present work the only pumping employed was that through the analyzer. The photoejected electrons are retarded and focused onto the 0.5-mm diameter entrance aperture with a three-element lens. The geometric acceptance angle of the analyzer is ca. 1×10^{-2} sr with electrons being detected at right angles to the direction of the beam of unpolarized photons. The relative intensities in our spectra cannot be directly interpreted as relative cross sections owing to (i) possible differences in the angular dependences of the orbital ionization cross sections (β factors) and (ii) the as yet undetermined analyzer transmission function. The He I photons are generated by a microwave discharge lamp operated with a He flow rate adjusted to achieve ca. 0.1-torr pressure in the discharge region. The discharge was maintained by a commercial radiotherm generator, which produces 100 W of 2.8-GHz microwave power. With this lamp and spectrometer the typical count rate on the Ar $^2P_{3/2}$ peak (15.94 eV binding energy) is 26 000 Hz with 30-meV fwhm resolution.

For the present work preliminary high-resolution (30-meV fwhm) PE studies on $Zr(BH_4)_4$ indicated that no sharp features (<0.1-eV fwhm) occurred. Thus the resolving power of the spectometer was degraded for this work by increasing the pass energy in the hemispheres from 2.0 to 6.0 eV. The spectra shown were obtained with a resolution of 0.1-eV fwhm (as measured on Ar). The energy scales were calibrated by recording the spectra with very small amounts of N_2 and Ar.

The tetrakis(tetrahydroborates) of Zr and Hf were prepared by reaction of the metal tetrahalides with lithium tetrahydroborate in ether followed by trap-to-trap distillation according to the procedure of James and Smith.[19] The samples were initially contaminated with diethyl ether; however, this was preferentially volatilized in the first few hours. The spectra shown were obtained after no detectable trace of diethyl ether remained (as indicated by the absence of its photoelectron band at 9.5 eV).

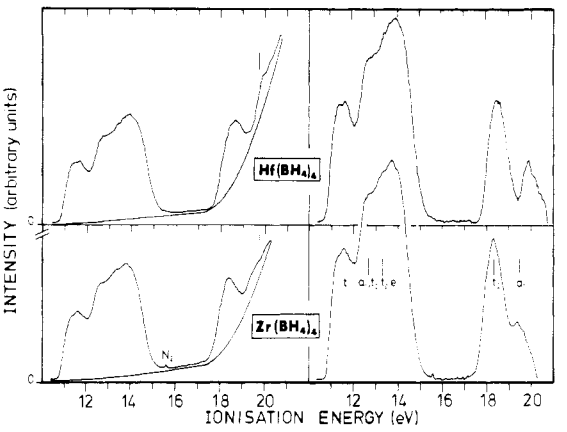

Figure 1. He I (21.2 eV) photoelectron spectra of $Hf(BH_4)_4$ and $Zr(BH_4)_4$. Spectra as recorded are shown in the left-hand panels along with the piecewise polynomial background subtracted to obtain the spectra shown in the right-hand panel. The vertical lines at 19.8 eV in the left-hand panels indicate the location of the $1a_1$ PE band of $Hf(BH_4)_4$.

Computational Details

$Zr(BH_4)_4$ was considered tetrahedral with regular T_d point group symmetry. The relevant interatomic distances were taken as those determined by gas-phase electron diffraction.[3] The quantum mechanical calculations were carried out with use of the discrete variational DV$X\alpha$ method of Baerends et al.[20] The valence orbitals [Zr (4d, 5s, 5p), B (2s, 2p), and H (1s)] were represented by a double-ζ STO basis while the core was kept frozen according to the procedure of Baerends et al.[21] A value of 0.7 was used for the exchange parameter. The ionization potentials were calculated with use of Slater's transition-state method.[22]

Results and Discussion

The photoelectron spectra as recorded are shown in the left-hand panels of Figure 1. The sloping backgrounds in the spectra arise from low-energy electrons, which are photoejected electrons inelastically scattered by gas molecules or the walls of the spectrometer. These backgrounds have been approxi-

(9) Ehemann, V. M.; Nöth, H. *Z. Anorg. Allg. Chem.* **1971**, *386*, 87.
(10) Marks, T. J.; Shimp, L. A. *J. Am. Chem. Soc.* **1972**, *94*, 1542.
(11) Sayer, B. G.; Thompson, J. I. A.; Nguyen Hao; Birchall, T.; Eaton, D. R.; McGlinchey, M. J. *Inorg. Chem.* **1981**, *20*, 3748.
(12) Wegner, P. A. "Boron Hydride Chemistry"; Muetterties, E. L.; Ed.; Academic Press: New York, 1973; Chapter 12.
(13) Marks, T. J.; Kolb, J. R. *Chem. Rev.* **1977**, *77*, 263.
(14) Andrews, M. A.; Bau, R.; Grynkewich, G. W.; Kirtley, S. W.; Marks, T. J.; Tipton, D. L.; Whittlesey, B. R. *J. Am. Chem. Soc.* **1977**, *99*, 7154.
(15) Downs, A. J.; Egdell, R. G.; Orchard, A. F.; Thomas, P. D. P. *J. Chem. Soc., Dalton Trans.* **1978**, 1755.
(16) Baerends, E. J.; Ros, P. *Int. J. Quantum Chem.* **1978**, *12*, 169.
(17) Baerends, E. J.; Ros, P. *Chem. Phys.* **1975**, *8*, 412.
(18) Frost, D. C.; Lee, S. F.; McDowell, C. A.; Westwood, N. P. C. *J. Electron. Spectrosc. Relat. Phenom.* **1977**, *12*, 95.
(19) James, B. D.; Smith, B. E. *Synth. React. Inorg. Met.-Org. Chem.* **1974**, *4*, 461.
(20) Baerends, E. J.; Ellis, D. E.; Ros, P. *Chem. Phys.* **1973**, *2*, 41.
(21) Baerends, E. J.; Ellis, D. E.; Ros, P. *Chem. Phys.* **1973**, *2*, 52.
(22) Slater, J. C.; *Adv. Quantum Chem.* **1972**, *6*, 1.

Table I. Vertical Ionization Energies (eV), Spectral Assignments, and Comparison to LCAO-HFS(DVXα) Calculations for $Zr(BH_4)_4$ and $Hf(BH_4)_4$

vertical energy (±0.1 eV)						
$Zr(BH_4)_4$		$Hf(BH_4)_4$		calcd energy	assigt[a]	
this work	ref 15	this work	ref 15	$Zr(BH_4)_4$	this work	ref 15
11.2	...	11.3	...		vibronic structure of $1t_1$	...
11.6	11.6	11.7	11.6	9.7	$1t_1$	$3t_2$, $2a_1$
12.7	12.7	12.6	12.6	10.8	$3t_2$	$1t_1$, $2t_2$, $1e$
				11.1	$2a_1$	
13.4	13.2	13.6	13.5	11.7	$2t_2$	
13.8	...	13.9	...	13.2	$1e$	
18.3	18.18	18.4	18.35	16.0	$1t_2$	$1t_2$
19.4	19.32	19.8	19.70	17.0	$1a_1$	$1a_1$

[a] Designation of the valence orbital from which the electron was ionized. The orbital numbering considers only the valence levels.

mated by piecewise polynomial curves, which have been subtracted from the recorded spectra to yield the difference spectra shown in the right-hand panels of Figure 1. The existence of the peaks at 19.8 eV (Hf) and 19.4 eV (Zr) was confirmed by a separate background subtraction procedure using the experimentally derived scattered background of an Ar spectrum. In addition, subsequent to the recording of the spectra presented in Figure 1 a photon beam dump was added to the spectrometer, which has removed the background of low-energy electrons from photoionization of the walls of the ionization region. The $Zr(BH_4)_4$ spectrum recorded with the modified apparatus is essentially identical with that shown in the right-hand panel of Figure 1. The energies of the spectral features and our proposed assignments are listed in Table I along with the results of the LCAO–HFS calculation on $Zr(BH_4)_4$ and a comparison with the results of Downs et al.[15]

With the exception of the band above 19 eV, the energies, relative intensities, and shapes of all of the photoelectron bands are virtually identical for these two molecules. The measured ionization energies agree within estimated errors (±0.1 eV) with those recorded earlier.[15] The similarity in the bonding and electronic structure of these two molecules evident from the comparison of their PE spectra is also reflected in their physical properties.[13] The origin of this of course is the lanthanide contraction, which is the reason that the size, polarizability, electronic structure, and chemistry of zirconium and hafnium are so remarkably similar.

Bonding in Tetrahedral d^0 Complexes. The electronic structure of the triply hydrogen-bridged $M(BH_4)_4$ species (M = Zr, Hf, U, Np) can be understood by an analogy with the electronic structure of classical tetrahedral d^0 complexes in which a central metal atom is surrounded by four monoatomic ligands. (An interesting empirical observation[23] related the parallelism between transition-metal borohydrides and the corresponding η^3-allyl systems.) The bonding in species such as MnO_4^- and $TiCl_4$ is described by interactions between the metal d orbitals (augmented by s and p orbitals) and symmetrized linear combinations of s, p_x, p_y, and p_z orbitals on the ligands. The symmetry-adapted linear combinations of atomic orbitals spanning the a_1, e, t_1, and t_2 representations of the T_d point group are shown in Table II.[24]

As outlined schematically in Figure 2, molecular orbital calculations on classical tetrahedral d^0 complexes reveal at low energy two orbital levels, $1a_1$ and $1t_2$, represented primarily by the s-ligand combinations α_2 and δ_1 (cf. Table II). At somewhat higher energy are the two orbitals responsible for the metal-ligand bonding in the complexes, $2t_2$ and 1e. The $2t_2$ orbital is a bonding linear combination between a δ_3 orbital

Table II. Symmetry Orbitals for Tetrahedral Complexes[a]

irreducible representations	metal	ligand
A_1	s (α_1)	$\{S_1 + S_2 + S_3 + S_4\}$ (α_2)
		$\{x_1 + y_1 + z_1 - x_2 - y_2 + z_2 + x_3 - y_3 - z_3 - x_4 + y_4 - z_4\}$ (α_3)
E	d_{z^2} (β_1)	$\{x_1 + y_1 - 2z_1 - x_2 - y_2 - 2z_2 + x_3 + y_3 + 2z_3 - x_4 + y_4 - 2z_4\}$ (β_2)
T_1		$\{x_1 - y_1 - x_2 + y_2 - x_3 - y_3 + x_4 - y_4\}$ (γ_1)
T_2		$\{s_1 - s_2 + s_3 - s_4\}$ (δ_1)
	p_x (δ_2)	$\{y_1 + z_1 + y_2 - z_2 - y_3 - z_3 - y_4 + z_4\}$ (δ_4)
	d_{yz} (δ_3)	$x_1 + x_2 + x_3 + x_4$ (δ_5)

[a] For the degenerate representations, only one component, e_a, t_{1x}, and t_{2x}, is shown. A right-handed coordinate system is assumed with the metal at the center and the four ligands at the following (x, y, z) positions: L_1 (a, a, a); L_2 (−a, −a, a); L_3 (a, −a, −a); L_4 (−a, a, −a).

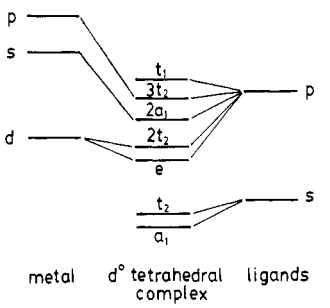

Figure 2. Molecular orbital scheme for classical d^0 tetrahedral complexes.

on the central atom and the δ_5 p-type ligand combination. In a similar way, 1e is a bonding combination between metal d (β_1) and ligand p (β_2) orbitals. These orbitals are shown in **1**.

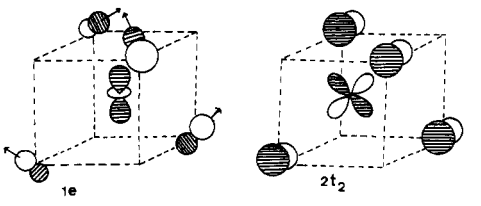

1

The three levels of highest energy have the designations $3t_2$, $2a_1$, and $1t_1$, respectively. Both $1t_1$ and $2a_1$ are nonbonding with respect to the central d orbitals for reasons of symmetry. The $3t_2$ orbital, represented primarily by the δ_4 p-type combination, is essentially nonbonding due to the small overlap

(23) Marks, T. J.; Kennelly, W. J.; Kolb, J. R.; Shimp, L. A. *Inorg. Chem.* **1972**, *11*, 2540.
(24) Ziegler, T.; Rauk, A.; Baerends, E. J. *Chem. Phys.* **1976**, *16*, 209.

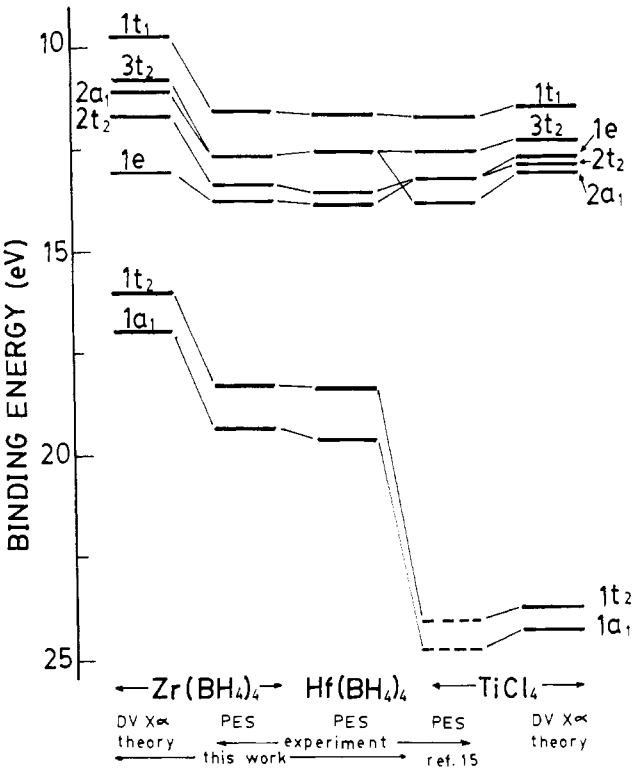

Figure 3. Correlation of experimental and theoretical orbital energies in $Zr(BH_4)_4$, $Hf(BH_4)_4$, and $TiCl_4$.

with the metal d orbital. These three orbitals are shown in **2**. The energy splitting between the t_1, $3t_2$, and $2a_1$ levels

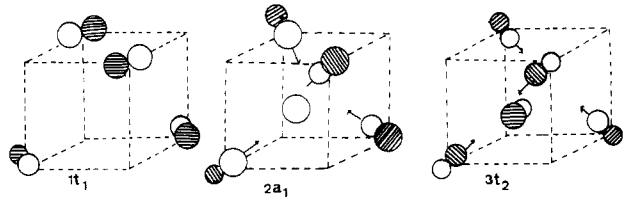

2

arises primarily from ligand–ligand interactions. However, weak interactions can occur between the metal atom and the $2a_1$ and $3t_2$ ligand orbitals since these orbitals can, depending on the central atom, interact with s- and p-type metal orbitals.

The BH_4^- fragment has eight valence electrons as do monatomic ligands such as Cl^- and O^{2-}. These electrons are in a_1 and t_2 orbitals of the tetrahedral BH_4^- fragment (**3**).

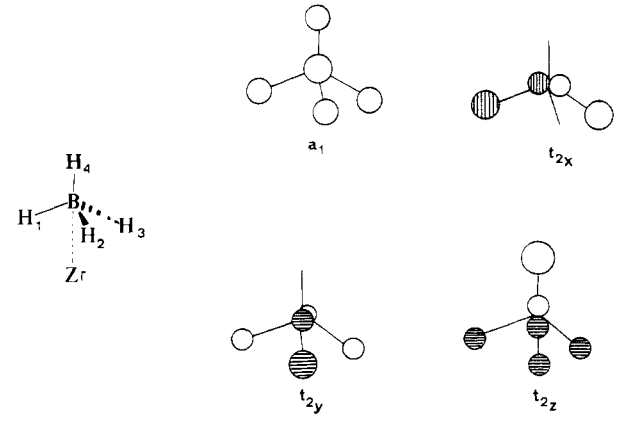

3

When coordinated to Zr in $Zr(BH_4)_4$, the a_1 and t_2 orbitals of BH_4^- have the same nodal properties as those of the s and p orbitals of monoatomic ligands. Symmetry combinations of a_1 on each BH_4^- fragment (mainly B 2s) give rise to group orbitals of a_1 and t_2 symmetry while symmetry combinations of the four t_2 orbitals give group orbitals with symmetry designations $t_1(1)$, $t_2(2)$, $a_1(1)$, and $e(1)$. This is exactly as in the case of monoatomic ligands (see Table II). Thus, the qualitative picture for the bonding in classical d^0 tetrahedral complexes, derived largely from orbital symmetries, should also apply to the isoelectronic systems $Zr(BH_4)_4$ and $Hf(BH_4)_4$. This has been a guiding principle for our spectral assignments. The correlation between the DVXα results for $Zr(BH_4)_4$, the experimental results for $Zr(BH_4)_4$ and $Hf(BH_4)_4$, and the theoretical and experimental orbital energies for $TiCl_4$[24] is shown in Figure 3.

The model for bonding in the triply coordinated tetrahydroborate d^0 metal complexes presented by Downs et al.[15] differs significantly from that just presented. Downs et al.[15] invoke a model of the electronic structure that is based on a division of the ligand MO's into σ-bridging types (those totally symmetric with respect to the M–B axis) and π-bridging types (those that contain the M–B axis in a nodal plane). We feel that this is an oversimplification especially with regard to the t_2 ligand MO's. The $2t_2$ (**1**) and $3t_2$ (**2**) orbitals are in fact combinations of both σ- and π-bridging orbitals. In particular the $2t_2$ orbital, which has maximum overlap with the metal d orbital, is described by a $(^2/_3)^{1/2}\pi - (^1/_3)^{1/2}\sigma$ combination whereas the $3t_2$ orbital, which has some overlap with the metal p orbital, is described by the $(^1/_3)^{1/2}\pi + (^2/_3)^{1/2}\sigma$ combination.[24] In addition to this qualitative difference in the model we reassign the ordering of the ligand orbitals. The differences between our assignments and those of Downs et al.[15] are discussed in the following section.

Spectral Analysis. The PE spectra can now be interpreted in light of the foregoing discussion and by comparison with the calculated energies. Both photoelectron spectra exhibit four distinct bands with the first and second bands containing structure. The first band in each spectrum (vertical IP of 11.6 eV; estimated adiabatic IP of 11.0 eV) corresponds to ionization of the t_1 level, a solely ligand-based B–H bonding orbital. This band exhibits a shoulder about 0.4 eV below the main peak maximum in each case. Although the 0.4-eV spacing is appropriate for one quantum of a B–H stretch mode, the absence of any further resolved vibronic levels suggests that the shoulder reflects change to a nontetrahedral geometry in the ion state, that is, a Jahn–Teller effect. Since all of the occupied orbitals are of bonding type—either metal–ligand (e, $2t_2$) or B–H bonding within the ligands (a_1, $1t_2$, $3t_2$, t_1)—the most stable ion-state geometries will differ from that of the ground state. Thus ionization will be accompanied by geometry changes leading to broad photoelectron bands. Excitation of a number of overlapping vibrational modes may explain the absence of resolved vibrational structure in any PE band. Alternatively, it is possible that some or all of the ion states of these molecules have dissociative potential curves.

The second band in the photoelectron spectrum has a distinct shoulder ca. 1.2 eV below the maximum and a second weak, but reproducible, shoulder about 0.4 eV below the peak maximum. Both the relative spacings predicted by the DVXα calculation and the qualitative discussion of the MO structure indicate that this region of the spectrum (12–14 eV) corresponds to ionization of the $2a_1$, $3t_2$ (ligand based orbitals) and the $2t_2$, 1e metal–ligand bonding orbitals. The ordering and relative spacings of these levels predicted in the $Zr(BH_4)_4$ calculation lead to an assignment of the $2a_1$ and $3t_2$ levels to the first shoulder (12.7 eV), the $2t_2$ level to the second (13.4 eV), and the peak maximum (13.8 eV) to the 1e level.

Our assignment of the metal–ligand bonding orbitals ($2t_2$, 1e) to the higher energy region of the second band (13–14 eV)

agrees with the earlier assignment of Downs et al.[15] It is strongly supported by the He II spectrum,[15] which shows an increase in the intensity of the 13–14-eV region relative to the first band (11.7 eV) and to the lower energy section of the second band as expected for MO's with metal d-orbital participation.

Our assignment differs in two aspects from that of Downs et al.[15] First, we reverse the ordering of the $1t_1$ and $3t_2$ levels; second, we place the $2a_1$ orbital in the second band while Downs et al.[15] assign it to the first band. Although the earlier assignments are also compatible with our model of the bonding in triply bridged tetrahydroborates, we consider our assignments to be more reasonable for the following reasons.

With regard to the $3t_2/1t_1$ ordering, we note that the DVXα calculation places the $1t_2$ orbital 1.1 eV below the $3t_2$ orbital. Since this method is known to give reliable orbital orderings[16] and since there is a relatively large difference in the calculated binding energies, we feel that the $1t_1$ ionization almost certainly corresponds to the first band. The correlation with the assigned theoretical[24] and experimental[34] orbital energies in $TiCl_4$ (Figure 3) further supports our assignment of $1t_1$ as the highest occupied molecular orbital of $Zr(BH_4)_4$.

With regard to the location of the $2a_1$ ionization, Downs et al.[15] claim that the relative intensities of the first and second bands are 1:2 and use this to support their assignment of $2a_1$ to the first band. Although arguments based on relative PES band intensities are generally inconclusive with regard to peak assignments (due to differences in angular distribution parameters, spectrometer transmission functions, and matrix elements for different ionizations) we note that the relative areas of the first and second bands are much closer to 1:3 than 1:2. This is in better agreement with our assignment (degeneracies of 1:3 for the first and second bands) rather than that of Downs et al.[15], which predicts a degeneracy ratio of 1:2. In addition, the DVXα calculation places the $2a_1$ level below the $3t_2$ level, which almost certainly must lie in the second band for intensity reasons.

The third and fourth bands at considerably higher ionization energies (18.3 and ca. 19.6 eV) are clearly the $1t_2$ and $1a_1$ levels, which are chiefly of B 2s character. For comparison, the B 2s levels of B_2H_6 lie at 16.0 and 22.3 eV.[25] The difference of 0.4 eV in measured energies of the B 2s a_1 levels of $Zr(BH_4)_4$ and $Hf(BH_4)_4$, which is detectable even in the unsubtracted spectra (see Figure 1), was also observed by Downs et al.[15] They suggest that the shift in the $1a_1$ level between zirconium and hafnium tetrakis(tetrahydroborates) reflects differences in direct metal–boron interactions. An appropriate probe for this would be a comparison of the NMR reduced coupling constants, $K_{^{91}Zr-^{11}B}$ and $K_{^{177}Hf-^{11}B}$. $J_{^{91}Zr-^{11}B}$ is 18 Hz,[11] but the Hf value is currently unknown. An alternate interpretation of the a_1 B 2s shift is possible.

The a_1 B 2s level can be regarded as having corelike properties. From this point of view its ionization potential could reflect the charge density at the boron atom more than interatomic overlap considerations. If the observed (small) difference is interpreted in this manner, the higher $1a_1$ IP of $Hf(BH_4)_4$ indicates a B 2s level less shielded from the boron nucleus and thus a somewhat lower electron density on B in $Hf(BH_4)_4$ than in $Zr(BH_4)_4$. This may also account for the 3-ppm difference in ^{11}B NMR chemical shifts of the two complexes.[1,11,26] However, this would attribute the whole shift to the diamagnetic term while the paramagnetic contribution is, perhaps unjustifiably, being ignored. Another way of looking at the interpretation of the a_1 B 2s shift is in terms of a less ionic ligand to metal bond in the hafnium than in the zirconium tetrakis(tetrahydroborate). (We note that the essentially covalent nature of these complexes is indicated by the calculated atomic charges of +0.5 (Zr), −0.5 (B), and +0.1 (H)).

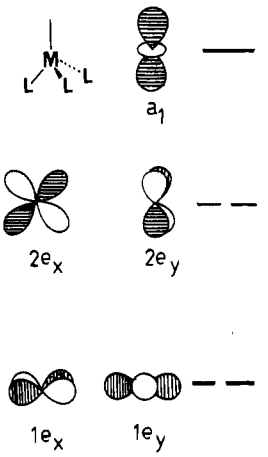

Figure 4. Symmetries of the d orbitals in an ML_3 fragment (C_{3v}).

On the Stability of the Tribridged Conformation. The stability of the triple hydrogen-bridged conformation relative to those of the double- or single-bridged conformations can be understood by considering the interaction of BH_4^- with the ZrX_3^+ fragment where X might be Cl^- or BH_4^-. The five unoccupied d levels are shown in Figure 4. In the triple-bridged conformation **4a**, the t_{2x}, t_{2y}, and t_{2z} orbitals of BH_4^-,

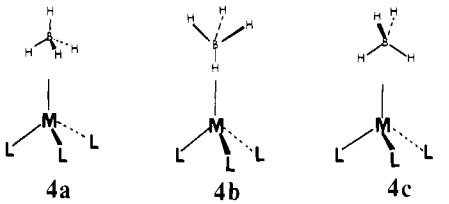

3, can interact with the $2e_x$, $2e_y$, and a_1 orbitals of ZrX_3^+ (Figure 3), thus giving rise to three bonding interactions.[27] In the monobridged conformation **4b**, there will only be one symmetry-allowed bonding interaction of any significance, that between the t_{2z} orbital of BH_4^- and the a_1 orbital of ZrX_3^+. This clearly indicates that **4a** will be appreciably more stable than **4b**. The possible dibridged conformation **4c** is finally considered. The three t_2 orbitals of BH_4^-, quantized along the C_2 axis of the ligand, are shown in **5**. Two strong bonding

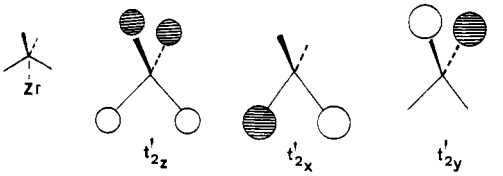

5

interactions are possible (as opposed to three in **4a**). One is between t'_{2z} and a_1 and the other between t'_{2x} and $2e_x$ (see **5** and Figure 4). In contrast, the interaction between t'_{2y} and $2e_y$ is negligible due to small overlaps. The better match between orbitals in **4a** should stabilize this conformation relative to **4c**. However, the absolute difference between **4a** and **4c** will depend on variations in the metal to hydrogen bond

(25) Brundle, C. R.; Robin, M. B.; Basch, H.; Pinsky, M.; Bond, A. *J. Am. Chem. Soc.* **1970**, *92*, 3863.

(26) It has been noted previously that correlations between PES data and ^{11}B NMR chemical shifts are not always readily apparent: Finn, P.; Jolly, W. L. *J. Am. Chem. Soc.* **1972**, *94*, 1540.

(27) A preliminary discussion of the bonding in transition-metal borohydrides has been published.[13] See also: Lauher, J. W.; Hoffmann, R. *J. Am. Chem. Soc.* **1976**, *98*, 1729.

distance. Finally, one should note that a possible contribution to the bonding from the relatively low-lying a_1 orbital of BH_4^- would be the same for all three conformations.

NMR studies of $Zr(BH_4)_4$ have shown that there is rapid exchange of the bridging and terminal hydrogens of each BH_4^- ligand.[1,10,11] The preceding discussion would suggest that a dibridged rather than a monobridged intermediate might be implicated, as shown in **6**. The actual difference in energy

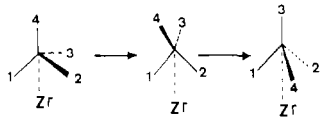

6

between **4a** and **4c** would then closely correspond to the experimentally observed activation energy (<5 kcal/mol) for the exchange process.[28] One should note that, for $Zr(BH_4)_4$, the Zr–H distance decreases to 1.88 Å in **4c** from 2.21 Å in **4a** if the Zr–B distance is constant. This shortened Zr–H distance will strengthen the bonding interactions in the dibridged species; thus this effect reduces the energy difference between **4a** and **4c** set by symmetry alone, and this could account for the small value of less than 5 kcal/mol for the activation energy of the exchange.

Monobridged and Dibridged Complexes of BH_4^-. In the d^0 metal fragment ZrX_3^+ all the metal orbitals were unoccupied; the overlaps between a_1, $2e_x$, and $2e_y$ on the fragment and t_{2x}, t_{2y}, and t_{2z} (all occupied) on BH_4^- consequently gave rise to three bonding interactions. If, however, the d levels are fully or partly occupied, these same overlaps might instead give rise to repulsive interactions between two occupied orbitals. For example, in the low-spin d^6 fragment of C_{4v} symmetry, **7**, d_{xy},

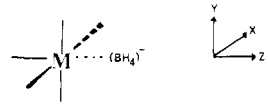

7

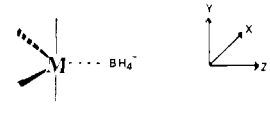

8

d_{xz}, and d_{yz} are occupied and d_{z^2} and $d_{x^2-y^2}$ are unoccupied. The mono-, di-, and tribridged conformations all have one bonding interaction involving d_{z^2} and t_{2z}. The dibridged conformation has in addition a repulsive interaction (d_{xz}, t_{2x}) while the tribridged BH_4^- unit has two repulsive interactions, d_{xz}, t_{2x} and d_{yz}, t_{2y}. One would thus anticipate the monobridged conformation to be more stable under these circumstances. Indeed, even though crystallographic data are lacking, the infrared spectra of the known d^6 complexes of the type $ML_5(BH_4)$, viz., $[(C_6H_{11})_3P]_2Ru(H)(CO)_2BH_4$ and $Mn(CO)_5BH_4$, indicate that the borohydride moieties are monobridged.[29,30]

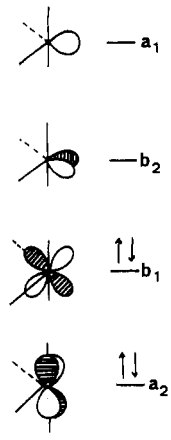

Figure 5. Symmetries of the orbitals in an ML_4 fragment (C_{2v}).

The dibridged mode has been documented by an X-ray diffraction study[14] on $[Mo(CO)_4(BH_4)]^-$. Here the d^6 metal fragment has C_{2v} symmetry (**8**). The electronic structure of ML_4 fragments with C_{2v} symmetry has been extensively studied.[31] The two highest occupied orbitals are shown in Figure 5. The a_1 orbital on ML_4 will give rise to a bonding interaction whether the borohydride moiety is mono-, di-, or tribridged. However, the triply bridged BH_4^- will in addition have a bonding interaction (b_2, t'_{2x}) and an antibonding interaction (b_1, t'_{2y}). The dibridged conformation is particularly interesting here. When the two ligating hydrogens are in the *xz* plane of **8**, an additional bonding interaction (b_2, t'_{2x}) is found; but, when the ligating hydrogens are in the *yz* plane, the π-type interaction (b_1, t'_{2y}) is anti-bonding. One can, therefore, predict that $[Mo(CO)_4BH_4]^-$ should exhibit a dibridged conformation with the two bonding hydrogens in the *xz* plane. This is indeed the case.[14]

Furthermore, one might expect that the destabilizing interaction when the BH_4^- moiety is rotated through 90° about the *z* axis would increase the activation energy for the exchange processes so prevalent in transition-metal borohydride chemistry. Gratifyingly, it is precisely in these d^6 cases that exchange can be made slow on the NMR time scale.[14,32]

As a final comment, it is noteworthy that the two d^6 systems $L_5M(BH_4)$ and $L_4M(BH_4)$ are respectively mono- and dibridged. This parallels the conversion of (η^1-allyl)$Mo(CO)_3C_5H_5$ to (η^3-allyl)$Mo(CO)_2C_5H_5$.[33] The analogous bonding patterns of borohydride and allyl ligands have been noted previously.[23]

Acknowledgment. This research has been financially supported by the Natural Sciences and Engineering Research Council of Canada (NSERC). A.P.H. gratefully acknowledges the support of an NSERC University fellowship. T.Z. acknowledges the support of an NSERC postdoctoral fellowship. We thank Dr. N. P. C. Westwood for his advice and assistance. Professor E. J. Baerends (The Free University, Amsterdam) kindly provided a copy of his HFS–DVM program system.

Registry No. $Zr(BH_4)_4$, 12370-59-1; $Hf(BH_4)_4$, 53608-70-1.

(28) Chuang, I.; Marks, T. J.; Kennelly, W. J.; Kolb, J. R. *J. Am. Chem. Soc.* **1977**, *99*, 7539.
(29) Holah, D. G.; Hughes, A. N.; Hui, B. C. *Can. J. Chem.* **1976**, *54*, 320.
(30) Bird, P. H.; Wallbridge, M. G. H. *Chem. Commun.* **1968**, 687.
(31) Rossi, A. R.; Hoffmann, R. *Inorg. Chem.* **1975**, *14*, 365.
(32) Empsall, H. D.; Mentzer, E.; Shaw, B. L. *J. Chem. Soc., Chem. Commun.* **1975**, 861.
(33) Green, M. L. H.; Stear, A. N. *J. Organomet. Chem.* **1964**, *1*, 230.
(34) Green, J. C.; Green, M. L. H.; Joachim, P. J.; Orchard, A. F.; Turner, D. W. *Philos. Trans. R. Soc. London, Ser. A* **1970**, *268*, 111.